Supporting Information

Castellano et al. 10.1073/pnas.1206446109

SI Materials and Methods

Aβ Preparation and Radioiodination. Amyloid-β 40 (Aβ40) peptide was synthesized by the Keck Foundation Biotechnology Resource Laboratory. Solid-phase Fmoc polypeptide synthesis was used to synthesize the Aβ peptide. Peptides were stored as lyophilized powder at −80 °C before use. Using the lactoperoxidase method (1), Aβ40 was iodinated with [^{125}I] and resolved by reverse-phase HPLC to separate the monoiodinated, nonoxidized form of Aβ from di-iodinated Aβ as well as nonlabeled, nonoxidized, and oxidized Aβ species, as confirmed previously (2–4), before assessing purity by MALDI-TOF mass spectrometry. We used reduced monoiodinated Aβ with specific activity of ∼60 μCi/μg (confirmed by MALDI-TOF mass spectrometry).

Brain Efflux Index Method. Stainless steel guide cannulae were stereotaxically implanted into the caudate-putamen of mice that had been anesthetized with ketamine (100 mg/kg) and xylazine (10 mg/kg). Coordinates for implantation were as follows: bregma –1.9 mm, 0.9 mm lateral from midline, 2.9 mm below dura. Following recovery from surgery to allow time for blood–brain barrier (BBB) repair for large molecules and before substantial chronic, reactive processes had occurred (2, 5–7), mice were coinjected with solution (0.5 μL) containing [^{14}C]inulin and [^{125}I]Aβ40 in artificial cerebrospinal fluid (CSF) into brain interstitial fluid (ISF) at 0.1 μL·min^{-1}. Mice were killed at various time points after injection (from 15 min to 150 min), and brains were immediately isolated and prepared for radioactivity analysis and TCA precipitation to analyze the molecular forms of tracer compounds, exactly as previously described (8, 9). For experiments to block LRP1-mediated clearance, mice were preinjected with α-LRP1 antibody (30 ng N20; Santa Cruz Biotechnology) over 5 min, followed by immediate coinjection of 12 nM [^{125}I]Aβ40 and [^{14}C]inulin and sacrifice after 90 min, exactly as described (9).

Brain Efflux Index Calculations and Analysis. Calculations were performed as previously described (2, 5, 8, 9). In brief, the percentage of [^{125}I]Aβ40 [corrected for degradation by trichloroacetic acid (TCA) precipitation analysis, as in earlier studies (2, 5, 8)] or [^{14}C]inulin remaining in brain at each time point following microinfusion was calculated as follows:

$$\%\ \text{recovery in brain} = 100 \times (N_b/N_i), \qquad \textbf{[S1]}$$

where N_b is the radioactivity of intact ligand remaining in brain upon conclusion of the experiment, and N_i is the initial amount of radioactive ligand injected into brain (in cpm for TCA-precipitable [^{125}I]Aβ40 and disintegrations per minute for [^{14}C]inulin). The rate of ISF bulk flow was determined as follows using the rate of clearance of inulin, an inert and polar reference molecule that neither transports across the BBB nor is retained in brain:

$$N_{\text{b,inulin}}/N_{\text{i,inulin}} = e^{-k_{inulin}t}, \qquad \textbf{[S2]}$$

where k_{inulin} indicates the rate of inulin clearance, and t denotes time. Based on our model (2, 8, 9), Aβ can be eliminated from the brain by BBB transport or elimination via ISF bulk flow into the CSF and cervical lymphatics. Our model incorporates retention within brain, i.e., binding of Aβ to receptors or chaperone molecules (i.e., various transport proteins), which may result in degradation or retention within the brain. Assuming a multiple time point efflux series with departure from linearity at later time points, the fraction of [^{125}I]Aβ40 remaining in the brain is expressed as follows:

$$N_{\text{b,Aβ}}/N_{\text{i,Aβ}} = (a_1 + a_2)e^{-k_1 t}, \qquad \textbf{[S3]}$$

where $a_1 = k_2/(k_1 + k_2)$ and $a_2 = k_1/(k_1 + k_2)$, and k_1 and k_2 denote fractional rate constants for total brain efflux and retention within brain, respectively. The sum of these fractions reduces to 1 by definition, given that they reflect fractions of total clearance and retention within the brain. Thus, Eq. **S3** describes the rate constant of total Aβ efflux from the brain, k_1. The fractional rate constant for Aβ clearance mediated by the BBB, k_3, can then be calculated as the difference between fractional rate constants for total efflux and ISF bulk flow:

$$k_3 = k_1 - k_{inulin}. \qquad \textbf{[S4]}$$

MLAB mathematical modeling (Civilized Software, Inc.) was used to fit the compartmental model to elimination data with inverse square weightage. Fractional rate constants were obtained by nonlinear regression curve fitting (GraphPad Prism 5.0), as we have described previously (2, 5, 8, 9).

In Vivo Microdialysis. Stereotaxic surgery and in vivo microdialysis was performed essentially as described (10, 11). Briefly, stereotaxic surgery was performed to implant guide cannulae in the caudal extent of hippocampus. A syringe pump (Stoelting) perfused 0.15% BSA (RPI) in artificial cerebrospinal fluid continuously at a flow rate of 1.0 μL·min^{-1} through an implanted 38-kDa molecular weight cutoff probe (BR-2; Bioanalytical Systems, Inc.) to dialyze ISF analytes collected every 60 min with a refrigerated fraction collector.

Quantitative Measurement of apoE, HJ5.1, and ISF Aβ. ApoE measurements were made by sensitive sandwich ELISA. Briefly, the mouse monoclonal antibody HJ6.2 was used for capture, and biotinylated mouse monoclonal antibody and HJ6.3 was used for detection of apoE standardized using pooled mouse plasma (C57BL/6J) (12). Concentration of biotinylated mouse monoclonal antibody HJ5.1, recovered from plasma or brain tissue, was assayed by ELISA. Samples were added to plates bound with a saturating amount of Aβ40 (50 ng·mL^{-1}) that had been captured by coated 3D6 antibody; biotinylated HJ5.1 was used to standardize concentration. Measurements of ISF [$A\beta_{1-x}$] from fractions collected during in vivo microdialysis were made by sandwich ELISA using synthetic Aβ40 as the standard (American Peptide). Briefly, plates were coated with m266 antibody (anti-$A\beta_{13-28}$), and bound Aβ was detected using biotinylated 3D6 antibody (anti-$A\beta_{1-5}$).

Confocal Microscopy Imaging. Overlap of HA-tagged low-density lipoprotein receptor (LDLR) transgene and BBB markers (CD31 or Aqp4) was assessed using anti-mouse HA antibody conjugated to Alexa 568 (1:200; Covance) and either rabbit anti-mouse AQP4 (1:500; Millipore) or rat anti-mouse CD31 (1:100; BD Pharmingen) antibodies. Fluorescently mounted tissue sections from TG mice corresponding to bregma −1.34 through −3.30 (each separated by 300 μm) were scanned with a Zeiss 510 confocal laser scanning microscope using a 488-nm argon laser for excitation of Alexa Fluor 488 (CD31/AQP4; emission collected through a 500- to 550-nm band-pass filter) and a 543 HeNe laser

for excitation of Alexa Fluor 568 (HA; emission collected through a 560- to 615-nm band-pass filter). Images were acquired from well-vascularized brain areas in an unbiased fashion. Brain sections from NTG littermates were completely devoid of HA signal.

Brain Tissue Processing and Quantification of Aβ/Amyloid Burden. Following transcardial perfusion with heparinized PBS, brains were removed and fixed in 4% (wt/vol) paraformaldehyde overnight, followed by immersion in 30% (wt/vol) sucrose. Brains were sectioned on a freezing-sliding microtome at a thickness of 50 μm. Coronal sections were collected from the rostral anterior commissure through the caudal extent of the hippocampus before staining with biotinylated 3D6 antibody (anti-$A\beta_{1-5}$) or X-34 dye. The NanoZoomer slide scanner system (Hamamatsu Photonics) was used to scan slides in batch mode, which allowed for the capture of images in brightfield (Aβ immunostaining) or fluorescent mode (X-34 staining). NDP viewer software was used to export acquired images from slides before quantitative analysis (ImageJ; National Institutes of Health). Three sections for each mouse, each separated by 300 μm (corresponding to bregma −1.7 mm, −2.0 mm, and −2.3 mm in mouse brain atlas), were used for determination of the percentage of area occupied by immunoreactive Aβ or amyloid burden (X-34–positive signal) in a blinded fashion. Slides were uniformly thresholded to minimize false-positive signal, as previously described (10, 11).

Biochemistry. After transcardial perfusion with heparinized PBS, brains were extracted, microdissected, and immediately frozen at −80 °C. For apoE ELISAs, hippocampal or cortical tissue was manually dounce-homogenized with 75 strokes in radioimmunoprecipitation assay buffer [50 mM Tris·HCl (pH 7.4), 150 mM NaCl, 0.25% deoxycholic acid, 1% Nonidet P-40, 1 mM EDTA] containing a mixture of protease inhibitors (Roche) or PBS containing mixture of protease inhibitors (Roche) for HJ5.1B ELISAs. Total protein concentration in brain homogenates was determined with a BCA protein assay kit (Pierce).

Surface Plasmon Resonance. Surface plasmon resonance (SPR) experiments were performed using a BIAcore 2000 instrument at 25 °C with CM5 GE-BIAcore sensor chips. Lyophilized Aβ(1–40) and Aβ(1–42) peptides were resuspended in trifluoroacetic acid, incubated at room temperature for 15 min, and dried under nitrogen gas before resuspending in hexafluoroisopropanol. Peptides were dried, resuspended, and aliquoted under nitrogen gas. The dry Aβ film was stored at −80 °C before use. DMSO was used to dissolve the dry Aβ film before immobilizing onto chip surface at densities of ∼4–5 fmol/mm^2 by amine coupling with sodium citrate buffer (pH 4.75; BIAcore AB). One flow cell was activated and blocked with 1 M ethanolamine (lacking protein), which was used as a control surface to normalize SPR signal from Aβ immobilized on flow cells. Experiments were conducted in PBS with 0.005% P20 (pH 7.4), and the analyte was injected at flow rate of 30 $\mu L \cdot min^{-1}$. Dissociation was followed in the same buffer for 15 min before regenerating the chip with 2 M guanidine-HCl/10 mM Tris·HC1 (pH 8.0) and washing with running buffer for 10 min before the next injection. Kinetic constants of binding were obtained using 1:1 Langmuir binding model using BIAevaluation software. Data are based on two independent measurements using six concentrations for each measurement.

Statistics. Unless indicated otherwise within figure legends, differences between groups were assessed using two-tailed Student's *t* test. For nonparametric distributions, a Mann–Whitney *U* test was performed. Measurements are reported as mean ± SEM. Analyses were performed using GraphPad Prism 5.0 software.

1. Thorell JI, Johansson BG (1971) Enzymatic iodination of polypeptides with 125I to high specific activity. *Biochim Biophys Acta* 251:363–369.
2. Bell RD, et al. (2007) Transport pathways for clearance of human Alzheimer's amyloid beta-peptide and apolipoproteins E and J in the mouse central nervous system. *J Cereb Blood Flow Metab* 27:909–918.
3. Deane R, et al. (2003) RAGE mediates amyloid-beta peptide transport across the blood-brain barrier and accumulation in brain. *Nat Med* 9:907–913.
4. LaRue B, et al. (2004) Method for measurement of the blood-brain barrier permeability in the perfused mouse brain: Application to amyloid-beta peptide in wild type and Alzheimer's Tg2576 mice. *J Neurosci Methods* 138:233–242.
5. Deane R, et al. (2004) LRP/amyloid beta-peptide interaction mediates differential brain efflux of Abeta isoforms. *Neuron* 43:333–344.
6. Deane R, et al. (2005) IgG-assisted age-dependent clearance of Alzheimer's amyloid beta peptide by the blood-brain barrier neonatal Fc receptor. *J Neurosci* 25: 11495–11503.
7. Cirrito JR, et al. (2003) In vivo assessment of brain interstitial fluid with microdialysis reveals plaque-associated changes in amyloid-beta metabolism and half-life. *J Neurosci* 23:8844–8853.
8. Shibata M, et al. (2000) Clearance of Alzheimer's amyloid-ss(1-40) peptide from brain by LDL receptor-related protein-1 at the blood-brain barrier. *J Clin Invest* 106:1489–1499.
9. Deane R, et al. (2008) apoE isoform-specific disruption of amyloid beta peptide clearance from mouse brain. *J Clin Invest* 118:4002–4013.
10. Kim J, et al. (2009) Overexpression of low-density lipoprotein receptor in the brain markedly inhibits amyloid deposition and increases extracellular A beta clearance. *Neuron* 64:632–644.
11. Castellano JM, et al. (2011) Human apoE isoforms differentially regulate brain amyloid-β peptide clearance. *Sci Transl Med* 3:89ra57.
12. Fryer JD, et al. (2005) The low density lipoprotein receptor regulates the level of central nervous system human and murine apolipoprotein E but does not modify amyloid plaque pathology in PDAPP mice. *J Biol Chem* 280:25754–25759.

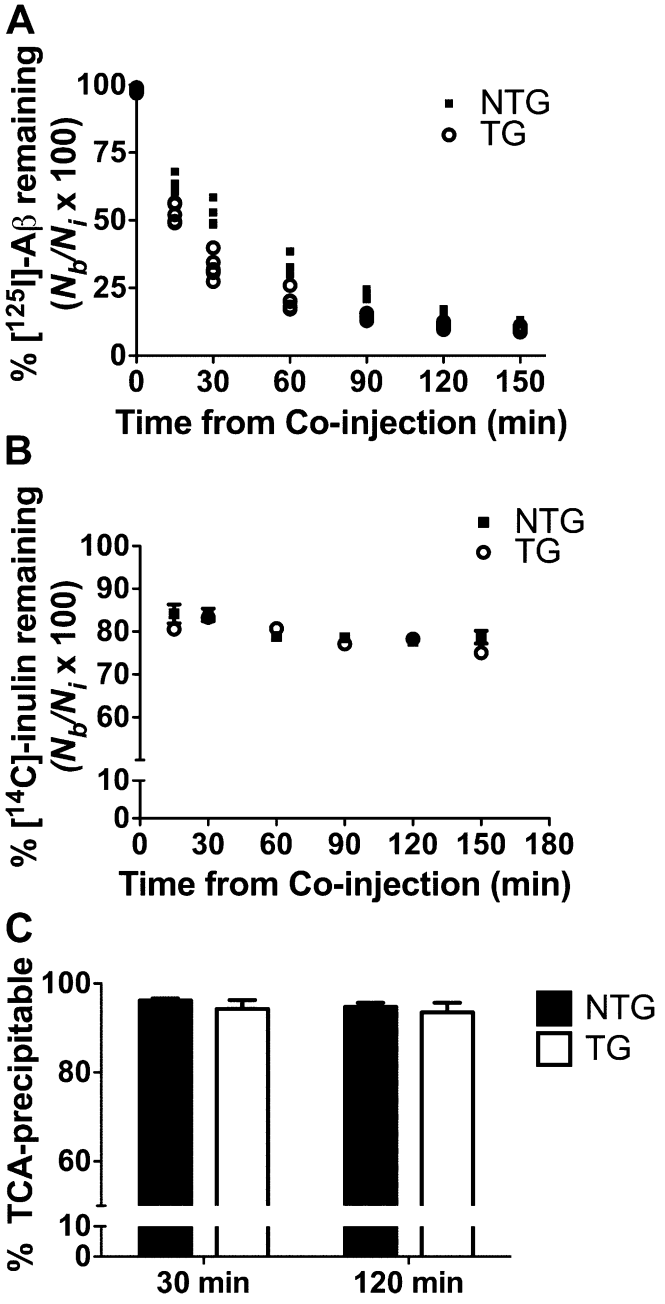

Fig. S1. LDLR overexpression does not appear to alter ISF bulk flow or the degradation of remaining [^{125}I]Aβ40. (*A*) The percentage of [^{125}I]Aβ40 remaining after microinjection into ISF of caudate-putamen in NTG (■) and TG (○) is represented as a scatterplot of the data from Fig. 1*A*. (*B*) Percentage remaining of coinjected [^{14}C]inulin over time course in experiments from *A* in NTG and TG mice. Time course includes 32–41 mice (n = 4–6 mice per time point for each group; 4–5 mo of age). (*C*) Percentage of remaining [^{125}I]Aβ40 that is precipitable by TCA (intact), representing intact peptide (n = 3–4 mice per time point for each group; 4–5 mo of age). Two-way ANOVA, with time and genotype as factors, revealed no significant differences among groups. Values represent mean ± SEM.

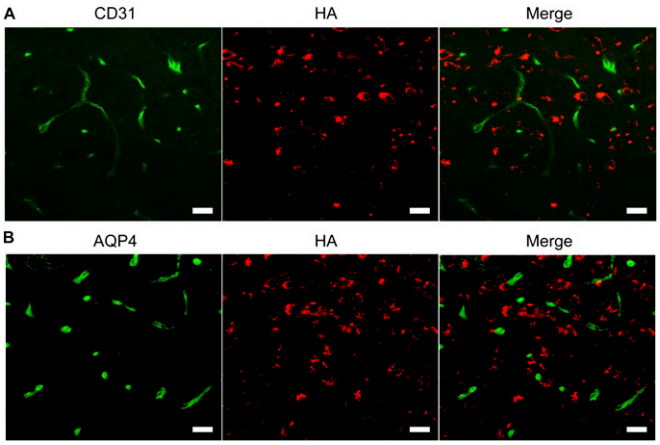

Fig. S2. LDLR transgene expression does not overlap with markers of the BBB. (*A*) Merge of confocal microscopy imaging of brain sections from 4- to 5-mo-old TG mice revealed no overlap in staining for the microvessel marker, CD31 (green), and HA-tagged LDLR transgene (red). (*B*) Lack of staining overlap between astrocytic endfeet marker, Aqp4 (green), and HA (red) from 4- to 5-mo-old TG brain sections. Representative images in *A* and *B* were selected from $n = 4$ per group. (Scale bars, 20 μm.)

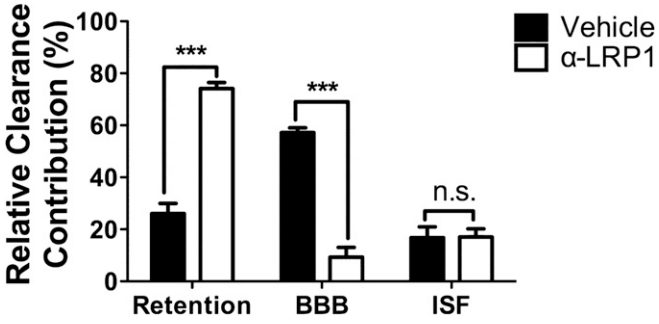

Fig. S3. Anti-LRP1 antibody (N20) blocks Aβ elimination from LDLR-TG brains. The relative clearance contributions of [^{125}I]Aβ40 by the BBB, ISF bulk flow, and retention within the brain were determined up to 90 min for 5- to 6-mo-old LDLR-TG (TG) mice given intracerebral microinjections of N20 α-LRP1 antibody (white bars) or vehicle (black bars) immediately before coinjection of [^{125}I]Aβ40 and [^{14}C]inulin ($n = 4$–5 mice per group), exactly as we have described previously (9). When two-way ANOVA was significant (with genotype and component as factors), differences among components were assessed using Tukey's post hoc test for multiple comparisons. ***$P < 0.001$; n.s., no significant difference between groups. Values represent mean ± SEM.

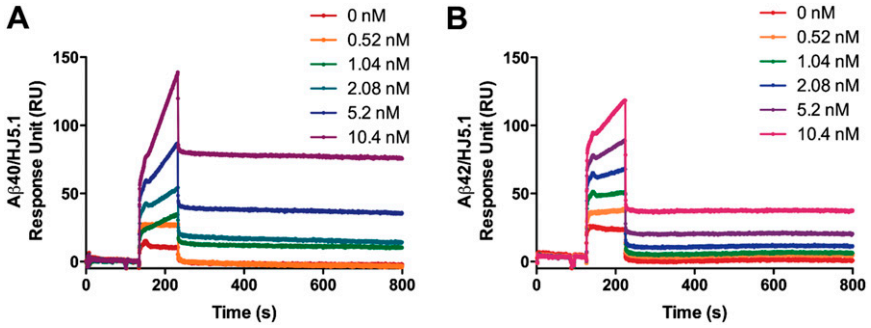

Fig. S4. Anti-Aβ antibody (HJ5.1) binds Aβ40 and Aβ42 with high affinity. (*A* and *B*) Representative sensograms from surface plasmon resonance experiments in which Aβ40 (*A*) or Aβ42 (*B*) was immobilized to the SPR chip before flowing different concentrations of HJ5.1 over the surface, which allowed for calculation of the dissociation constant for the interaction (K_d).

Table S1. Fractional rate constants (k, min^{-1}) for [^{125}I]Aβ40 and [^{14}C]inulin following coinjection in TG and NTG mice

Constants	TG k, min^{-1}	NTG k, min^{-1}
Total efflux (k_1)	0.03326 ± 0.00428	0.01885 ± 0.00202
BBB transport (k_3)	0.03081 ± 0.00472	0.01652 ± 0.00245
ISF bulk flow (k_{inulin})	0.00244 ± 0.00045	0.00232 ± 0.00043
Brain retention (k_2)	0.01278 ± 0.00085	0.02664 ± 0.00605

Values represent mean ± SEM from n = 32–41 mice per group.

Table S2. Intravenously administered biotinylated HJ5.1 enters the CNS at low levels

Concentration	Hippocampus	Cortex
[HJ5.1B] ng/mg tissue	0.248 ± 0.0144	0.280 ± 0.0116
% of HJ5.1 injected	$2.65 \times 10^{-3} \pm 4.36 \times 10^{-4}$	$1.75 \times 10^{-2} \pm 6.70 \times 10^{-4}$

Concentration of biotinylated HJ5.1 (HJ5.1B) in hippocampal or cortical homogenates from PDAPP$^{+/-}$ mice killed 120 min following injection, as determined by sensitive sandwich ELISA (n = 4; 3–4 mo old). Values represent means ± SEM.